Agriculture, Ecosystems and Environment 301 (2020) 107027

Contents lists available at ScienceDirect

Agriculture, Ecosystems and Environment

journal homepage: www.elsevier.com/locate/agee

Carbon-nitrogen isotope coupling of soil organic matter in a karst region under land use change, Southwest China

Guilin Han[a,*], Yang Tang[b], Man Liu[a], Lukas Van Zwieten[c], Xiaomin Yang[d], Changxun Yu[e], Hailong Wang[f,g], Zhaoliang Song[d,*]

[a] Institute of Earth Sciences, China University of Geosciences (Beijing), Beijing 100083, PR China
[b] The State Key Laboratory of Environmental Geochemistry, Institute of Geochemistry, Chinese Academy of Sciences, Guiyang 550002, PR China
[c] New South Wales Department of Primary Industries, 1243 Bruxner Highway, Wollongbar, NSW 2477, Australia
[d] Institute of Surface-Earth System Science, Tianjin University, Tianjin 300072, PR China
[e] Department of Biology and Environmental Science, Linnaeus University, SE-39182 Kalmar, Sweden
[f] School of Environment and Chemical Engineering, Foshan University, Foshan, Guangdong 528000, PR China
[g] Key Laboratory of Soil Contamination Bioremediation of Zhejiang Province, Zhejiang A & F University, Hangzhou, Zhejiang 311300, PR China

ARTICLE INFO

Keywords:
Soil organic carbon and nitrogen
$\delta^{13}C$
$\delta^{15}N$
Land use change
SW China

ABSTRACT

The soil stable carbon (C) and nitrogen (N) isotopes are widely used to indicate C_3/C_4 vegetation history, N sources and transformation processes, respectively. However, land use change, particularly converting forest into farm land, alters soil organic matter (SOM) sources and processes in soils, resulting in a hard understanding of soil C and N fate. In the present study, soil organic carbon (SOC) and soil organic nitrogen (SON) contents, and their stable isotope compositions ($\delta^{13}C$ and $\delta^{15}N$) were determined in the five soil profiles under land use change (i.e., conversion of native forest land into shrub land, grass land, maize field, and paddy land) in Lobo county, Guizhou province, Southwest China. A coupling of ^{13}C and ^{15}N isotope in SOM under land use change was verified whether it could provide more accurate indications of sources and transformation processes.

The SOC and SON contents of native forest land at the 0 ~ 20 cm depth were significantly larger than these under other transformed lands. The SOC and SON contents decreased exponentially with increasing soil depth under all land use types, and showed opposite trends with soil pH. The C/N ratios of SOM in the soils under undisturbed native forest decreased from 10 to 7 with increasing soil depth, while an irregular fluctuation along soil profile was shown in other transformed lands. Similarly to the most study in the soils under C_3 forest, the $\delta^{13}C$ and $\delta^{15}N$ values of SOM in the soils under native forest at the 0 ~ 50 cm depth increased with increasing soil depth, with the range of −27.7‰ ~ −25.7‰ and 6.5‰ ~ 10.0‰, respectively. While decreasing trends of them in the soils below 50 cm depth were attributed to the mixing of ^{13}C and ^{15}N-depleted organic matters from bedrocks. However, the $\delta^{13}C$ and $\delta^{15}N$ values of SOM along the soil profiles under other transformed lands were intensively irregularly fluctuated between −29.1‰ and −19.0‰, 1.2‰ and 7.9‰, respectively. The single $\delta^{13}C$ and $\delta^{15}N$ signals in the soil profiles of transformed lands indeed revealed the alterations of historical C_3/C_4 composition and N transformation processes after land use change, but these indications were not specific. The result of the coupling of ^{13}C and ^{15}N isotope under native forest land reveals a positive relationship between them, which associated with full plant-absorption against ^{15}N-depleted inorganic nitrogen derived from SOM mineralization. This study suggests that the coupling of C−N isotope fractionation more likely occurs in the C_3 forest ecosystem with high N utilization efficiency. However, the replacement of native forest by farm land or grass land will reduce soil N utilization efficiency.

1. Introduction

Ever-increasing population stress increases the requirement of food from the agroecosystem (Amundson et al., 2015); one measure is to expand the area of cultivable land by deforestation. However, the conversion of native forest land to farm land leads to the loss of soil carbon and other nutrients, and soil degradation (Smith et al., 2016). Since soil organic carbon (SOC) and soil organic nitrogen (SON) are essential factors for agricultural production and climate changes, understanding the biogeochemical cycling of these two nutrients is

* Corresponding author.
E-mail addresses: hanguilin@cugb.edu.cn (G. Han), zhaoliang.song@tju.edu.cn (Z. Song).

https://doi.org/10.1016/j.agee.2020.107027
Received 10 March 2020; Received in revised form 10 May 2020; Accepted 21 May 2020
Available online 31 May 2020

essential to the global biogeochemical cycles (Schmidt et al., 2011; Wang et al., 2014). Most previous studies on land use change have focused on soil organic matter (SOM) because of its importance for sustainable crop production and its measurable response to changes in global climate change and land use management (Chen et al., 2002; Rasmussen, 2006; Liu et al., 2014; Zhang et al., 2014). Several studies have shown that land use changes have reduced soil nutrient levels, including SOC and SON content, and altered their transformation processes (Zhang et al., 2013; Gao et al., 2014; Oktaba et al., 2014; Wang et al., 2014; Gelaw et al., 2015; Bojko and Kabala, 2017). The importance of studying the spatial and temporal variations of SOC and SON due to global environmental concerns has been highlighted by Navas et al. (2012). Generally, SOC and SON contents are suggested to be higher in forest soils than in agricultural or pastureland soils (Rumpel and Kogel-Knabner, 2011; Trumbore et al., 1995). While Gao et al. (2014) reported that both density and storage of soil C and N were significantly higher in croplands and orchards than those in forest lands in subtropical regions of China. Tesfaye et al. (2016) reported that land use types and soil depth are important factors influencing SOC and SON turnover. However, whether and how land use types affect the stoichiometry of soil nutrients remain unclear (Deng and Shangguan, 2017; Liu et al., 2017). Besides, human activities, such as fertilizer application, have increased N input in agroecosystems, potentially disrupting the natural cycling of C through influencing multiple processes such as plant net primary production and microbial activities (Gallowy et al., 2005; Templer et al., 2007). Hence, it is necessary to further understand the response of agroecosystems to changes in C and N cycles.

Natural stable isotopes can be used as tracers and proxies of ecological processes, with an advantage being the relatively low cost and the convenience of measurement compared to other techniques, such as artificial stable-isotope labeling and radioisotope dating (Templer et al., 2007). Stable C isotope ($\delta^{13}C$) have increasingly been used to estimate soil C turnover, assess the decomposition rate of SOC, and reconstruct historical changes of C_3 and C_4 vegetation (Boutton et al., 1998; Neff et al., 2002; Staddon, 2004; Krull et al., 2006; Peri et al., 2012). Stable N isotopes ($\delta^{15}N$) can indicate N source in agroecosystems when the dominant N processes in soil are known, for example, $\delta^{15}N$ of fertilizer is near 0‰; 3‰ ~ 14‰ in manure (Choi et al., 2017). Nadelhoffer and Fry (1988) suggested that N is largely bound to organic materials in surface soils, whereas inorganic N becomes relatively important at specific depths where the content of organic N declines. Many studies suggested that $\delta^{15}N$ of SON is controlled by nitrification and denitrification, the adsorption of ammonium (NH_4^+) on clays, and the leaching of nitrate (NO_3^-) (Mariotti et al., 1981; Hogberg and Johannisson, 1993; Portl et al., 2007). Hogberg (1997) suggested that soil N transformation processes discriminate against the heavier stable isotope of ^{15}N enrichment of the residual substrates. However, land use change will alternate soil C and N sources and their transformation processes, and there has been a challenge to understand soil C and N fate by single stable C and N isotope signals (Choi et al., 2017). Although the coupling of $\delta^{13}C$ and $\delta^{15}N$ in soil profile has been used to indicate SOM turnover rate under mature C_3 forest (Peri et al., 2012), in the present study, whether the coupling of them can provide more accurate indications of sources and transformation processes under land use change was verified.

Guizhou Province is located in Southwest China and has the largest karst area in the world (Zeng et al., 2020b). Karstification in the region is very developed and the karst types are the most diverse compared to other karst area in the world. This region currently faces many environmental problems (Zeng et al., 2019; Han et al., 2019), in particular water and soil loss, which is commonly accompanied by soil nutrient depletion. Serious water and soil loss have led to a rapid expansion of rocky desertification, which has caused multiple environmental and social issues in Guizhou Province (Wang et al., 2004; Zhang et al., 2019). The SOC contents and $\delta^{13}C$ compositions in this area were investigated to estimate the contribution of C_3/C_4 vegetation to SOC (Han et al., 2015) and SOM stabilization within aggregates (Liu et al., 2019a, b; Liu et al., 2020). While the current study aims to understand the mechanisms of C-N isotope coupling. Therefore, this study investigated the coupling of $\delta^{13}C$ and $\delta^{15}N$ in the soil profiles under land use change in the typical karst forest region of southwest China. The aim of this study was (1) to understand the vertical distribution characteristics of SOC and SON content and their stable isotope composition ($\delta^{13}C$ and $\delta^{15}N$); (2) to determine whether single $\delta^{13}C$ and $\delta^{15}N$ signature can effectively reveal the history of C_3 and C_4 vegetation and indicate N sources and transformation processes under land use change; (3) to identify the indications of SOM sources and transformation processes by C-N isotope coupling under land use change.

2. Sampling site and analysis methods

2.1. Study area and site characteristics

This study focused on variations in the concentration of SOC and SON, and their stable isotopic composition in soil profiles under land use change. In October 2013, five soil profiles under different types of land use were collected from Maolan National Natural Reserve Park in Libo county, Guizhou province, Southwest China (Fig. 1). The five soil profiles were classified as native forest land (LBF), shrub land (LBS), grass land (LBG), paddy land (LBP), and maize field (LBM), in which the first two capital letters (LB) of naming abbreviations of the soil profiles mean the location of sampling site in Libo county, the third capital letter means the type of land use. The original vegetation of all five profiles was the native forest. In the 1960s, many original forests were deforested using for the development of agriculture and graziery, and these areas gradually developed to shrub land, grass land, and farm land. The native forest land, shrub land, and paddy land mainly supported C_3 plants, while the maize field and grass land were dominantly C_4 plants. The study area is controlled by a subtropical monsoonal climate, with the mean annual air temperature of 15.3 °C and the mean annual precipitation of 1750 mm (Zeng et al., 2020a). The lithology of the study area is mainly limestone, dolomite and little sandstone. Detailed site descriptions are given in Table 1.

2.2. Soil sampling and analysis

The paddy soil samples were collected after the rice harvest. At each site, soil samples were collected at depth intervals of 10 cm from the soil surface to the weathered parent material. A total of 52 soil samples were collected from the five soil profiles under the different land uses (Table 2). Soil samples were air-dried at 40 °C in an oven, then removed roots and plant debris and passed through 2 mm sifter.

Soil pH (soil/water of 1/2.5) was measured using a pH meter, with a precision of ± 0.05 (Liu et al., 2019b). After soil samples were finely ground (< 149 μm), the pulverous samples were treated with 0.5 mol·L^{-1} HCl at room temperature for 24 h to remove carbonates (Midwood and Boutton, 1998), washed to neutrality (pH = 7) using pure water (18.2 MΩ cm), centrifuged, then dried at 60 °C and stored for subsequent analysis. Similarly, inorganic N, including NO_3^- and NH_4^+, were removed using 2 mol L^{-1} potassium chloride (KCl) for 24 h (Meng et al., 2005). Thus, the soil samples C and N left behind would have been mainly composed of SOC and SON. The organic C and N content in the treated soils was measured using an elemental analyzer (EA: PE2400, Perkin Elmer, Waltham, MA, USA), with a precision of ≤ 0.01%. The actual SOC and SON contents should be calibrated due to loss of inorganic C and N (Liu et al., 2019b).

Stable isotopes of SOC and SON were measured using an isotope ratio mass spectrometer (Finnigan™ MAT-252, Thermo Fisher Scientific, Waltham, MA, USA) coupled to the EA via a Conflo-III universal interface in the State Key Laboratory of Environmental Geochemistry, affiliated to the Institute of Geochemistry (IGC), the Chinese Academy of Sciences (CAS). Measurements were normalized based on the

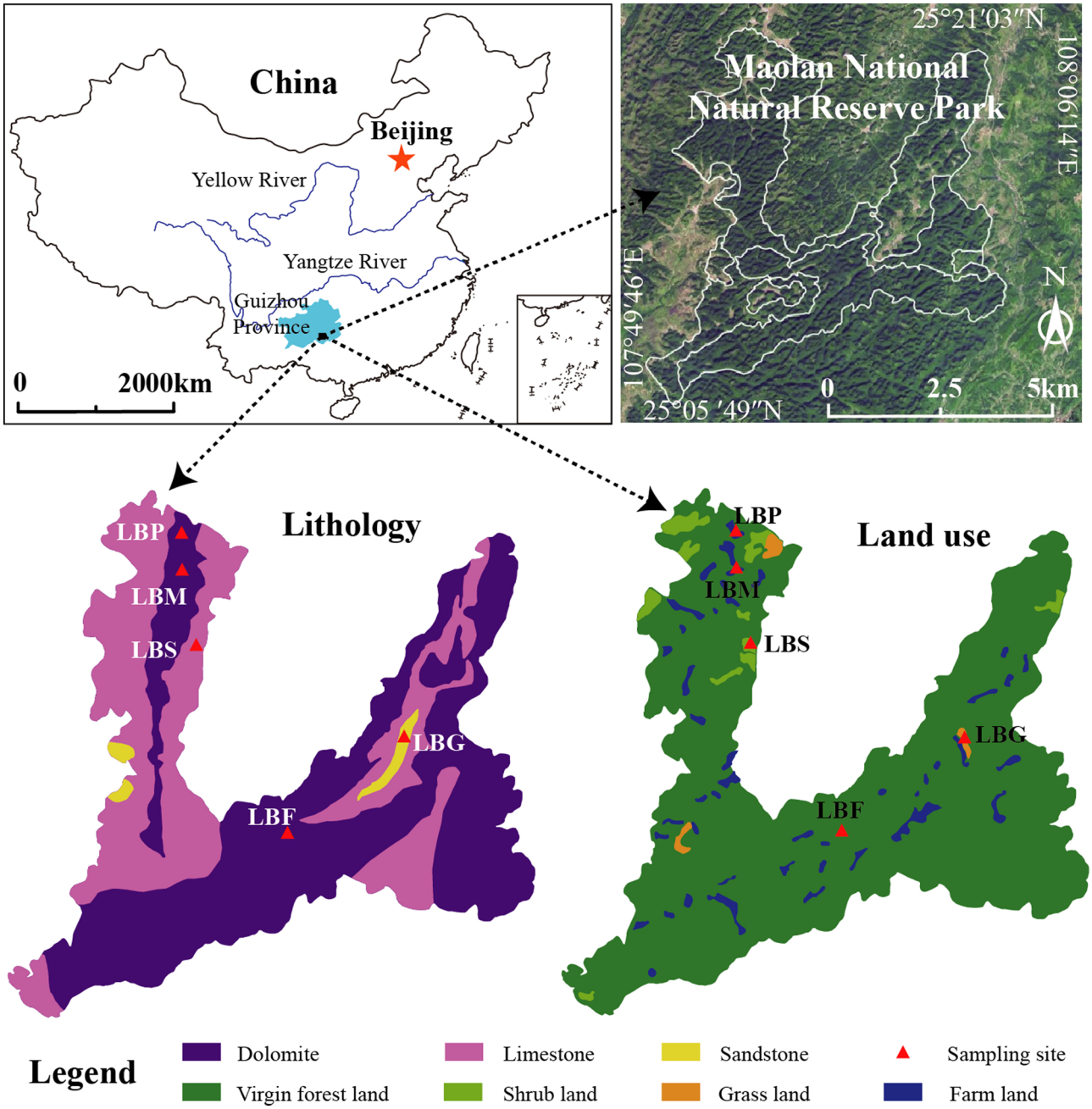

Fig. 1. Location of study area and sampling sites. LBF, the site in native forest land; LBG, the site in grass land; LBS, the site in shrub land; LBM, the site in maize land; LBP, the site in paddy land. The satellite imagery was obtained using Google Earth software. The boundary of Maolan National Natural Reserve Park was determined in ArcGIS software.

measured values of standards (IAEA N-1; IAEA C_3), corrected for internal and procedural blanks, and reported in $\delta^{13}C$ and $\delta^{15}N$ notation relative to Vienna Pee Dee Belemnite (V-PDB) and air per mil, where:

$$\delta^{13}C(‰) = [(R_{sample} - R_{V\text{-}PDB})/R_{V\text{-}PDB}] \times 1000, \text{ where } R = {}^{13}C/{}^{12}C \quad (1)$$

$$\delta^{15}N(‰) = [(R_{sample} - R_{air})/R_{air}] \times 1000, \text{ where } R = {}^{15}N/{}^{14}N \quad (2)$$

Routine $\delta^{13}C$ and $\delta^{15}N$ measurements were conducted with an overall precision of ± 0.1‰ and ± 0.2‰, respectively. Each sample was run in duplicate, and the results indicated that the differences were within the range of measurement accuracy based on the measurement values of standard material.

2.3. Statistical analysis

One-way ANOVA analysis with least significant difference (LSD) test was performed to determine the significance of land use types on SOC and SON content in the 0 ~ 20 cm depth soil layer at the level of $P < 0.05$. The relationships between SOC (or SON content) and soil depth (or soil pH) were determined by nonlinear regression analysis. The relationships between the $\delta^{13}C$ and $\delta^{15}N$ of SOM in the five soil profiles at the 0 ~ 50 cm depth were determined by linear regression analysis. The outliers were deleted after detecting by Box-plot, then the best-fit lines were drawn, and equation, coefficient r, and P-value were determined. Statistical analyses were performed by SPSS 18.0 (SPSS Inc., Chicago, IL, USA) and figures were done by SigmaPlot 12.5 (Systat Software GmbH, Erkrath, Germany).

Table 1
Visible characteristic of the five soil profiles.

Profile	Sample site	Above sea level	Profile thickness	Parent material	Land use history	Dominant vegetable species	Visible characteristics
LBF	25°12′7″N 107°59′43″E	582 m	90 cm	Dolomite	Native forest land	Dominated by C_3 vegetation: *Rosa cymosa; Lindera communis; Pyracantha fortuneana; Selaginella tamariscina; Castanopsis tibetana*	0–20 cm: black, humus layer, abundant plant roots ; 20–60 cm: black brown soil, tight, few plant roots ; 60–90 cm: gray limestone soil, tight; Connecting the bedrock
LBG	25°15′07″N 108°02′20″E	557 m	100 cm	Sandstone	Alteration of native forest to grass land for 50 years	Dominated by C_4 vegetation: *Miscanthus floridulus; Imperata cylindrical*	0–30 cm: black gray clay, few plant roots, tight ; 30–60 cm: yellow clay, a small amount of stones ; 60–100 cm: brown soil at the bottom of the gravel layer
LBS	25°17′15″N 107°58′04″E	548 m	90 cm	Limestone	Alteration of native forest to shrub land for 60 years	*Pyracantha fortuneana* (C3); *Miscanthus sinensis* (C4)	0–10 cm: black, rich in humus ; 10–30 cm: black brown soil, few plant roots ; 30–60 cm: brown gray clay, tight ; 60–90 cm: black clay, tight; Connecting the bedrock
LBM	25°19′41″N 107°56′36″E	541 m	100 cm	Dolomite	Alteration of native forest to maize field for 30 years	*Zea mays* (C_4)	0–10 cm: Black gray clay, with abundant plant roots ; 10–30 cm: gray black and yellow clay, tight, few root ; 30–60 cm: gray and black clay, tight; 60–90 cm: yellow brown clay, tight
LBP	25°20′21″N 107°57′40″E	539 m	90 cm	Dolomite	Alteration of native forest to paddy land for 30 years	*Oryza sativa* (C_3)	0–30 cm: gray clay; 30–0 cm: brick red clay, tight; 60–90 cm: gray clay, a small amount of yellow soil, tight; Connecting the bedrock

3. Results

3.1. Distribution of SOC and SON contents, C/N ratio and soil pH

The SOC contents varied from 0.23% to 7.89% (Table 2), and were the highest in the topsoil of the LBF profile. In the soils at the 0 ~ 20 cm depth, the contents of SOC were significantly higher in virgin forest land compared with grass land and farm land, while were slightly higher than shrub land, and the contents in grass land and farm lands were not different (Fig. 2A). For the soils below 20 cm depth, SOC contents in all soil profiles were commonly less than 2%, and became stable with soil depth (Fig. 3A). From the maximal SOC content in the topsoil, the SOC content decreased exponentially with depth by regression analysis (Fig. 3A).

The SON contents of all soil samples varied from 0.08% to 0.75% (Table 2), with similar depth distribution as that of SOC (Fig. 3B). Similarly, the SON contents in virgin forest land were significantly larger than those in grass land and farm land, while were slightly larger than that in shrub land, and the contents in grass land and farm lands were not different (Fig. 2B). The SON contents in all soil profiles also decreased exponentially with depth, and were commonly less than 0.2% in the soils below 20 cm depth (Fig. 3B).

The C/N ratios in SOM of all soil samples ranged between 1 and 16 (Table 2). On the whole, the C/N ratios in the five soil profiles displayed a decreasing trend from the surface to the bottom of the profile (Fig. 4B). Only in the soil profile (LBF) under virgin forest land, the C/N ratios steadily decreased with increasing soil depth from 10 to 7. There are many abnormal ups and downs in the intermediate of other soil profiles. For example, abnormal ups occurred in the LBG profile at 20 ~ 30 cm depth; in the LBS profile at 10 cm depth; in the LBP profile at 10 and 50 cm depth and in the LBM profile at 60 ~ 90 cm depth. Abnormal downs occurred in the LBP profile at 30 cm depth. The C/N ratio generally decreases with increasing of SOM age in soils (Conen et al., 2008). These results showed the dislocation of different decomposition degree SOM in soil profiles after land use change.

Soil pH of all soil samples ranged between 6.5 and 7.8 (Table 2), and it generally increased with depth in all soil profiles (Fig. 4A). The soil samples in the LBM profile had relatively high pH values, which varied from 7.2–7.8. An inverse relationship was observed between SOC, SON, and soil pH, with a lower SOC and SON content corresponding to higher pH values of these karst soils (Fig. 5A and B).

3.2. The $\delta^{13}C$ and $\delta^{15}N$ values of SOM

The $\delta^{13}C$ values of the topsoil from the LBF, LBG, LBS, LBP, and LBM profiles were −27.7‰, −22.8‰, −25.8‰, −24.4‰, and −23.9‰, respectively (Fig. 6A). In the soils at the top 20 cm, $\delta^{13}C$ values of the five profiles increased by 2‰ ~ 5‰. Vertical changes in $\delta^{13}C$ were less than 2‰ under virgin forest land (LBF), while changed by 6‰ ~ 11‰ through soil profiles under other land use. For all soil samples of all soil profiles, the most negative $\delta^{13}C$ values (−29.5‰ ~ −27.1‰) occurred in the LBS profile at the 40 ~ 80 cm depth, LBM profile at the 70 ~ 90 cm depth, and LBF profile at the 60 ~ 80 cm depth.

The $\delta^{15}N$ values of the topsoil from the LBF, LBG, LBS, LBP, and LBM profiles were 6.5‰, 3.4‰, 4.9‰, 5.8‰, and 5.2‰, respectively (Fig. 6B). Most soil samples in the LBF profile had relatively large $\delta^{15}N$ values near 10‰. Except in the LBS profile, vertical changes in $\delta^{15}N$ values with depth in the other four profiles were less than 4‰. For all soil samples of all soil profiles, the most negative $\delta^{15}N$ values (1.2‰ ~ 2.3‰) occurred in the LBS profile at 20, 40, and 50 cm depth.

4. Discussion

4.1. Effects of land use change on SOC and SON contents in soil profiles

Previous studies of SOM revealed that the profile change in its

Table 2
Soil pH, SOC and SON content and their isotopic compositions, and C/N ratio in the five soil profiles.

Profiles	Depth (cm)	pH	SOC (%)	$\delta^{13}C$ (‰)	SON (%)	$\delta^{15}N$ (‰)	C/N	Profiles	Depth (cm)	pH	SOC (%)
LBF	0	6.5	7.89	–27.7	0.75	6.5	10.48	**LBP**	0	7.6	1.74
	–10	6.7	4.06	–26.3	0.47	9.1	8.69		–10	7.3	1.07
	–20	6.7	2.41	–26.0	0.29	9.8	8.33		–20	7.3	0.56
	–30	6.6	1.64	–25.9	0.20	9.8	8.16		–30	7.2	0.44
	–40	6.5	1.14	–26.5	0.16	9.5	6.98		–40	7.4	0.36
	–50	6.7	1.33	–25.7	0.18	10.0	7.42		–50	7.5	0.23
	–60	6.7	1.14	–26.9	0.16	9.9	7.25		–60	7.6	0.42
	–70	6.8	1.03	–27.2	0.14	6.5	7.28		–70	7.5	0.77
	–80	6.9	0.88	–27.5	0.13	9.6	7.01		–80	7.7	0.87
	–90	7.0	0.91	–26.5	0.13	8.9	7.12		–90	7.8	0.66
	Min	**6.5**	**0.88**	**–27.7**	**0.13**	**6.5**	**6.98**		**Min**	**7.2**	**0.23**
	MAX	**7.0**	**7.89**	**–25.7**	**0.75**	**10.0**	**10.48**		**MAX**	**7.8**	**1.74**
	Average	**6.7**	**2.24**	**–26.6**	**0.26**	**9.0**	**7.87**		**Average**	**7.5**	**0.71**
	SD	**0.2**	**2.21**	**0.7**	**0.20**	**1.3**	**1.10**		**SD**	**0.2**	**0.44**
LBM	0	6.7	2.37	–24.4	0.23	5.8	10.15	**LBG**	0	6.6	2.24
	–10	6.8	2.06	–24.1	0.15	5.5	13.39		–10	6.7	2.05
	–20	6.8	1.11	–21.6	0.14	6.0	7.72		–20	6.9	1.98
	–30	6.8	0.80	–19.9	0.20	3.1	4.07		–30	7.0	1.84
	–40	6.9	1.82	–19.4	0.19	6.4	9.60		–40	6.9	0.57
	–50	6.8	1.72	–21.8	0.14	5.7	12.14		–50	7.0	0.75
	–60	6.9	0.97	–22.8	0.13	7.3	7.22		–60	7.1	0.30
	–70	7.0	0.89	–21.3	0.15	5.0	6.03		–70	7.1	0.43
	–80	7.0	1.19	–22.5	0.15	7.9	7.80		–80	7.2	0.27
	–90	6.9	1.03	–25.7	0.15	6.1	6.70		–90	7.2	0.23
	–100	6.8	1.15	–21.0	0.23	4.6	5.03		–100	7.5	0.34
	Min	**6.7**	**0.80**	**–25.7**	**0.13**	**3.1**	**4.07**		**Min**	**6.6**	**0.23**
	MAX	**7.0**	**2.37**	**–19.4**	**0.23**	**7.9**	**13.39**		**MAX**	**7.5**	**2.24**
	Average	**6.9**	**1.37**	**–22.2**	**0.17**	**5.8**	**8.17**		**Average**	**7.0**	**1.00**
	SD	**0.1**	**0.53**	**1.9**	**0.04**	**1.3**	**2.89**		**SD**	**0.3**	**0.83**

Profiles	$\delta^{13}C$ (‰)	SON (%)	$\delta^{15}N$ (‰)	C/N	Profiles	Depth (cm)	pH	SOC (%)	$\delta^{13}C$ (‰)	SON (%)	$\delta^{15}N$ (‰)	C/N
LBF	–23.9	0.22	5.2	8.04	**LBS**	0	6.6	4.71	–25.8	0.48	4.9	9.76
	–19.0	0.14	5.1	7.90		–10	6.5	4.41	–24.8	0.28	5.8	15.97
	–20.3	0.12	3.7	4.68		–20	6.5	2.24	–22.3	0.23	2.0	9.82
	–20.2	0.11	4.9	4.11		–30	6.6	1.73	–20.9	0.20	6.8	8.63
	–19.4	0.11	4.0	3.43		–40	6.8	1.34	–27.2	0.14	2.3	9.88
	–22.4	0.10	3.9	2.29		–50	6.8	0.61	–28.6	0.13	1.2	4.57
	–25.4	0.11	5.1	3.93		–60	7.1	0.57	–27.8	0.12	5.6	4.82
	–28.8	0.11	5.0	6.86		–70	7.0	0.70	–28.2	0.11	5.9	6.49
	–29.5	0.12	5.0	7.18		–80	7.3	0.58	–29.1	0.11	5.9	5.11
	–27.4	0.11	5.4	5.97		–90	7.5	0.71	–21.4	0.36	4.4	1.97
	–29.5	**0.10**	**3.7**	**2.29**		**Min**	**6.5**	**0.57**	**–29.1**	**0.11**	**1.2**	**1.97**
	–19.0	**0.22**	**5.4**	**8.04**		**MAX**	**7.5**	**4.71**	**–20.9**	**0.48**	**6.8**	**15.97**
	–23.6	**0.12**	**4.7**	**5.44**		**Average**	**6.9**	**1.76**	**–25.6**	**0.22**	**4.5**	**7.70**
	4.0	**0.03**	**0.6**	**2.02**		**SD**	**0.4**	**1.58**	**3.1**	**0.13**	**2.0**	**3.97**

(*continued on next page*)

Table 2 (*continued*)

Profiles	$\delta^{13}C$ (‰)	SON (%)	$\delta^{15}N$ (‰)	C/N	Profiles	Depth (cm)	pH	SOC (%)	$\delta^{13}C$ (‰)	SON (%)	$\delta^{15}N$ (‰)	C/N
LBM	–22.8	0.16	5.8	14.01								
	–22.3	0.16	6.5	12.64								
	–19.5	0.13	6.0	15.32								
	–22.3	0.13	6.3	14.24								
	–22.3	0.11	4.6	5.43								
	–22.9	0.11	4.9	6.73								
	–21.6	0.08	3.8	3.51								
	–22.5	0.08	4.5	5.46								
	–26.0	0.10	4.5	2.84								
	–23.3	0.24	4.0	0.96								
	–21.2	0.20	3.4	1.66								
	–26.0	**0.08**	**3.4**	**0.96**								
	–19.5	**0.24**	**6.5**	**15.32**								
	–22.4	**0.14**	**4.9**	**7.53**								
	1.6	**0.05**	**1.1**	**5.47**								

Note: SOC, soil organic carbon; SON, soil organic nitrogen; SOM, soil organic matter; LBF, the site in native forest land; LBG, the site in grass land; LBS, the site in shrub land; LBM, the site in maize land; LBP, the site in paddy land.

content depends mainly on the plant functional type (Han et al., 2015, 2017). Generally, plant biomass decreased as deforestation, and shrub land has more vegetation cover than farm land. Differences in plant biomass in different land use type directly affect organic matter input into soils through plant litter and root exudate (Jobbagy and Jackson, 2000). Rate of SOM input into the soil is reduced when the land use changes from native forest to grass land and farm land consistent with previous studies (Aryal et al., 2018; Smith et al., 2016; Lal, 2004). Long-term tillage significantly reduces soil microbe quantity and destroy soil aggregates resulting in more rapid SOM decomposition (Liu et al., 2019a). These differences in input and decomposition of SOM determine the role of land use types on SOC and SON contents, similar to this study that the contents decreased as follows: virgin forest land > shrub land > grass land and farm land (Fig. 2). Effects of land use types on SOM content mainly occur at the top 20 cm soil layer, where is the main area of the root distribution, soil microbe, and tillage (Chaopricha and Marín-Spiotta, 2014). While root density, organic matter input, and microbial activities will be restricted in the soil layer below 20 cm depth under all land use types. These results show that the conversion of forest land to grass land or farm land significantly reduces SOM content in the surface soils.

In the forest region of Maolan, subtropical, monsoonal and humid climate is benefited for accumulation of plant biomass, which provides an abundant organic matrix for soil microorganism metabolism in topsoil (National Soil Survey Office National Soil Survey Office (NSSO, 1998). On the other hand, soil microbes under this climate are more active than in more dry and cold region. While in soils below 20 cm depth, SOM that mainly derived from plant litters and soil microbe continuously decreased with increasing depth (Fierer et al., 2003; Chen et al., 2005), resulting in exponentially decreasing SOC and SON along with soil depth from the topsoil to the bottom of the profiles (Fig. 3). In higher pH calcareous soils, humus combines with calcium ion to form organic-inorganic complexes, which improve SOM accumulation (Zhu and Liu, 2006). While SOM content was the largest when soil pH decreased to 6.5 in this study (Fig. 5), likely related to the accumulation of humic acid. Soil pH increased with depth (Fig. 4A), likely resulting from neutralization by humic acid in topsoil and decreased loss of carbonate minerals in deeper soils.

4.2. Restricted utilization of single $\delta^{13}C$ and $\delta^{15}N$ of SOM in soil profiles to indicate their sources and processes under land use change

The decreasing C/N ratio with soil depth generally reflects the degree of decomposition of SOM (Nadelhoffer and Fry, 1988; Krull et al., 2006). C/N ratio stably increased with depth in LBF profile, while it irregularly varied in other four profiles that occurred land use change (Fig. 4B). These results suggested that the decomposition degree of SOM was likely not corresponding with the depth of it located. This inference was confirmed through vertical changes in $\delta^{13}C$ of SOM (Fig. 6). Soil $\delta^{13}C$ values of SOM mainly depend on organic matter input from C_3 and C_4 vegetation; therefore the $\delta^{13}C$ values of SOM can be used to distinguish SOC contribution from C_3 and C_4 plants (Han et al., 2015). Only in the LBF profile, $\delta^{13}C$ values varied in a small range at –28‰ ~ –26‰ (Fig. 6A), which indicated that SOM derived from C_3 vegetation. While in the other four profiles, vertical changes in $\delta^{13}C$ values were irregular with a ranged from –30‰ to –19‰ (Fig. 6A). In the study area, due to the dislocation of different decomposition degree SOM in soil profiles after land use change, changes in $\delta^{13}C$ values along a soil profiles could not be used to indicate the history of C_3/C_4 vegetation in the land that occurred land use change. Furthermore, the $\delta^{13}C$ values of SOM in the bottom of the LBF, LBS and LBM profiles ranged from −27.1‰ to −29.5‰ (Fig. 6 A), which were close to the value (−28‰) of organic matter contained in bedrock (Liu et al., 2020). The mixing effect of organic carbon derived from bedrock and modern plant leads to promiscuous $\delta^{13}C$ value in deep soils, which also hinders the indication of C_3/C_4 vegetation history by profile $\delta^{13}C$ values (Boutton

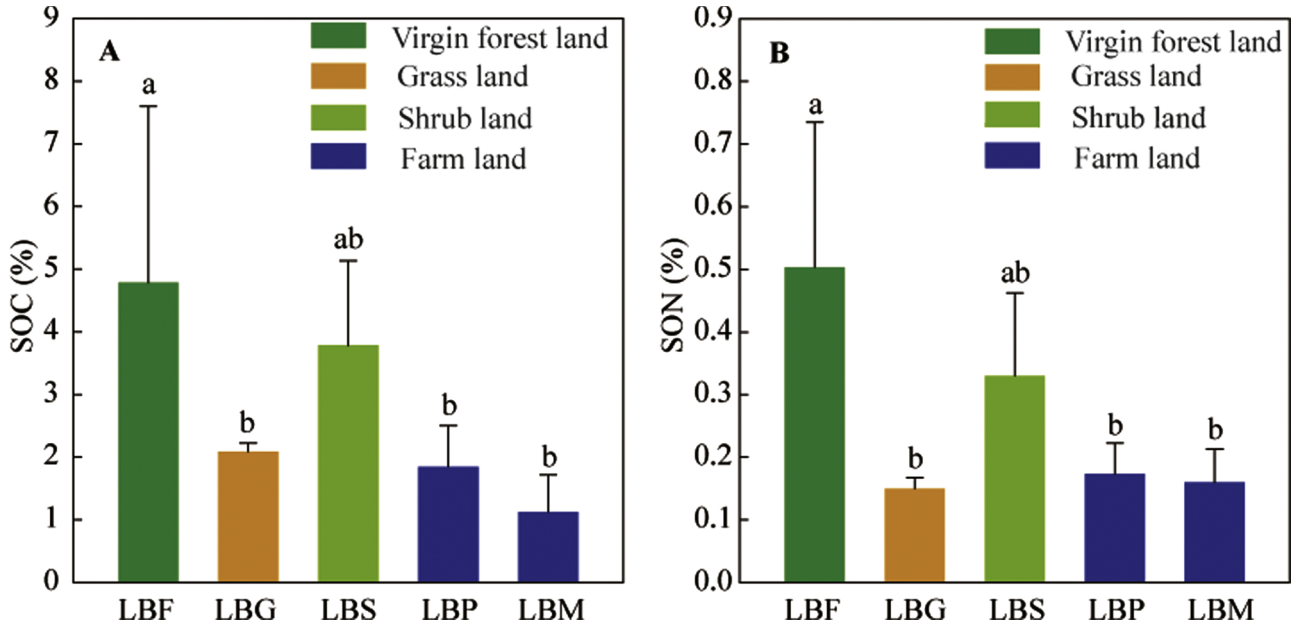

Fig. 2. Average SOC (A) and SON (B) contents in 0 ~ 20 cm depth soils of the five soil profiles. SOC, soil organic carbon; SON, soil organic nitrogen; LBF, the site in native forest land; LBG, the site in grass land; LBS, the site in shrub land; LBM, the site in maize land; LBP, the site in paddy land. Different lowercase letters indicate significant differences of SOC content (or SON content) among different sites at $P < 0.05$ level based on the least significant difference (LSD) test.

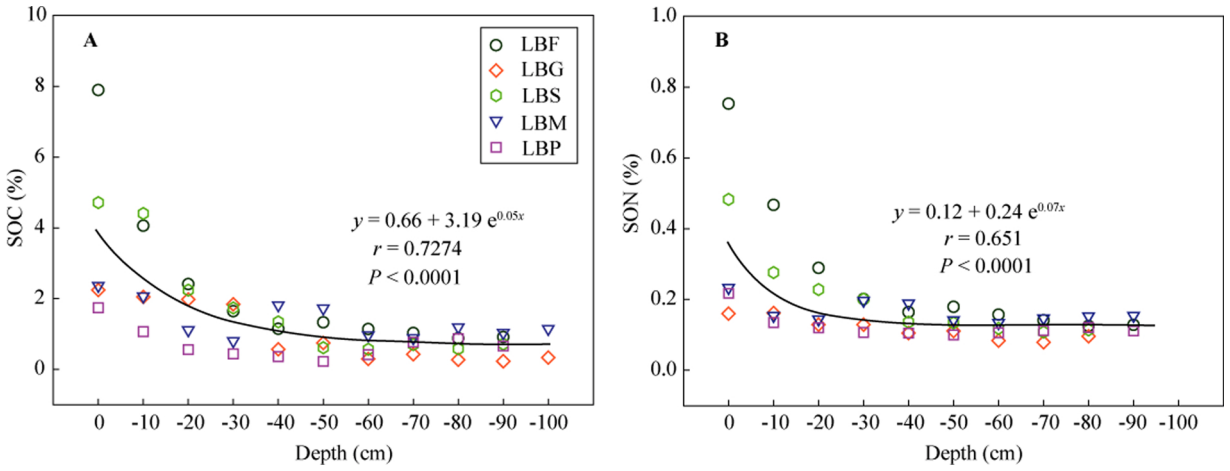

Fig. 3. Changes in SOC (A) and SON (B) along soil depth in the five soil profiles. SOC, soil organic carbon; SON, soil organic nitrogen; LBF, the site in native forest land; LBG, the site in grass land; LBS, the site in shrub land; LBM, the site in maize land; LBP, the site in paddy land. The outliers derived from SON content these were deleted after detecting by Box-plot.

et al., 1998; Neff et al., 2002; Staddon, 2004; Krull et al., 2006; Peri et al., 2012).

Soil $\delta^{15}N$ values depend on $\delta^{15}N$ composition of inputs, including litter and fertilizer, and $\delta^{15}N$ fractionation in transformation processes between different N compounds (Mariotti, 1983; Houlton et al., 2006; Hobbie and Hogberg, 2012; Hilton et al., 2013). The $\delta^{15}N$ values of SOM at topsoil of the five soil profiles were almost same with a ranged from 5‰ to 6‰ (Fig. 6B), which mainly were controlled by $\delta^{15}N$ composition of leaves (Nel et al., 2018). In undisturbed native forest land, the $\delta^{15}N$ values of SOM in the LBF profile at the 0 ~ 50 cm depth increased with increasing soil depth (Fig. 6B), resulting from ^{15}N enrichment in microbe in SOM decomposition process and root uptake of ^{15}N-depleted NO_3^- after nitrification (Mariotti, 1983; Hobbie and Hogberg, 2012). While decreasing trend in the soils below 50 cm depth attribute to the mixing of ^{15}N-depleted organic matters from bedrocks (−3.2‰ to −1.3‰, unpublished data). The $\delta^{15}N$ values of SOM along the soil profiles under other transformed lands (LBS, LBG, LBM, and LBP) were intensively irregularly fluctuated between 1.2‰ and 7.9‰, which were controlled by the alteration of N transformation processes under land use change. These N transformation processes, including ammonification, microbial immobilization, nitrification and denitrification, are associated with different types of fungi. Microbial quantity and species are significantly diverse in the soils at different land use types (Wallander et al., 2009). Therefore N transformation processes will adjust after land use change. Although the higher $\delta^{15}N$ values of SOM in deep soils are linked to the loss of ^{15}N-depleted NO_3^- which derived from the nitrification process in many studies (Nadelhoffer and Fry, 1988; Krull et al., 2006). This irregular fluctuation in $\delta^{15}N$ values along with soil profiles did not explicitly indicate a specific N transformation processes in the land that occurred land use change.

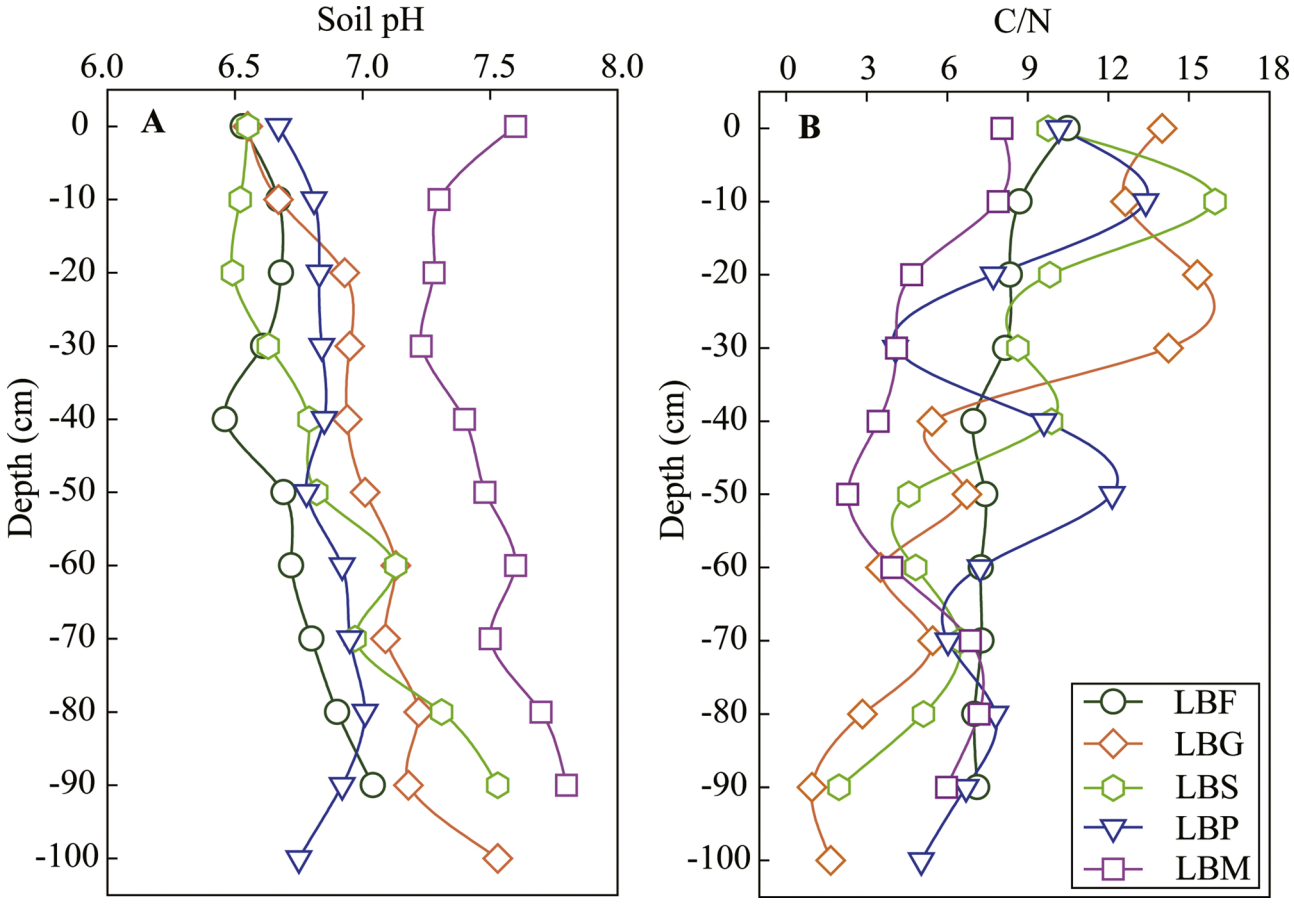

Fig. 4. Changes in soil pH (A) and C/N ratio of SOM (B) along soil depth in the five soil profiles. SOM, soil organic matter; LBF, the site in native forest land; LBG, the site in grass land; LBS, the site in shrub land; LBM, the site in maize land; LBP, the site in paddy land.

4.3. Coupling of C-N isotope fractionation

For the karst soils under land use change, single $\delta^{13}C$ values of SOM in profile did not indicate the transformation and translocation processes of SOM, due to the alteration of C_3/C_4 vegetation composition and the mixing effect of organic carbon derived from bedrock and modern plant as above mentioned. Similarly, single $\delta^{15}N$ values also did not indicate these soil N processes due to the changes in fertilizer application and $\delta^{15}N$ fractionation in N transformation processes under land use change. Therefore, a coupled relationship between the $\delta^{13}C$ and $\delta^{15}N$ of SOM was determined in the present study to identify the transformation and translocation processes of SOM under land use change (Fig. 7). The $\delta^{13}C$ values in the deep soils were strongly affected by the mixing effect; thus soils at the 0 ~ 50 cm depth were selected to analyze the relationship. From the topsoil at 0 cm depth to the soil at 50 cm depth, the $\delta^{13}C$ values of SOM in the LBF profile which was located in native forest land increased by 2‰, while they in other profiles that had occurred land use change increased by 4‰ ~ 8‰ (Fig. 7). The

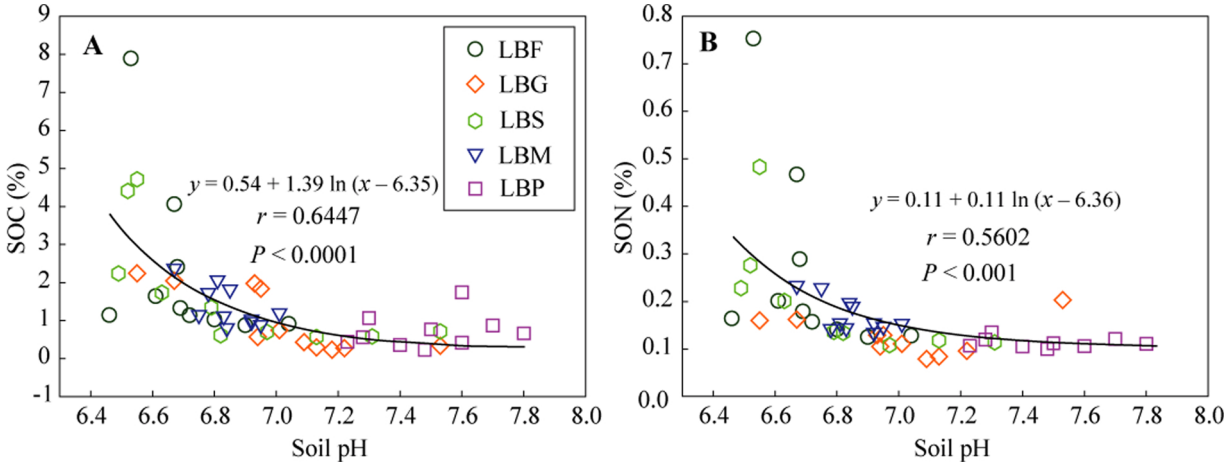

Fig. 5. Relationships between the soil pH and SOC content (A), SON content (B) in the all depth soils from the five soil profiles. SOC, soil organic carbon; SON, soil organic nitrogen; LBF, the site in native forest land; LBG, the site in grass land; LBS, the site in shrub land; LBM, the site in maize land; LBP, the site in paddy land. The outliers derived from SON content these were deleted after detecting by Box-plot.

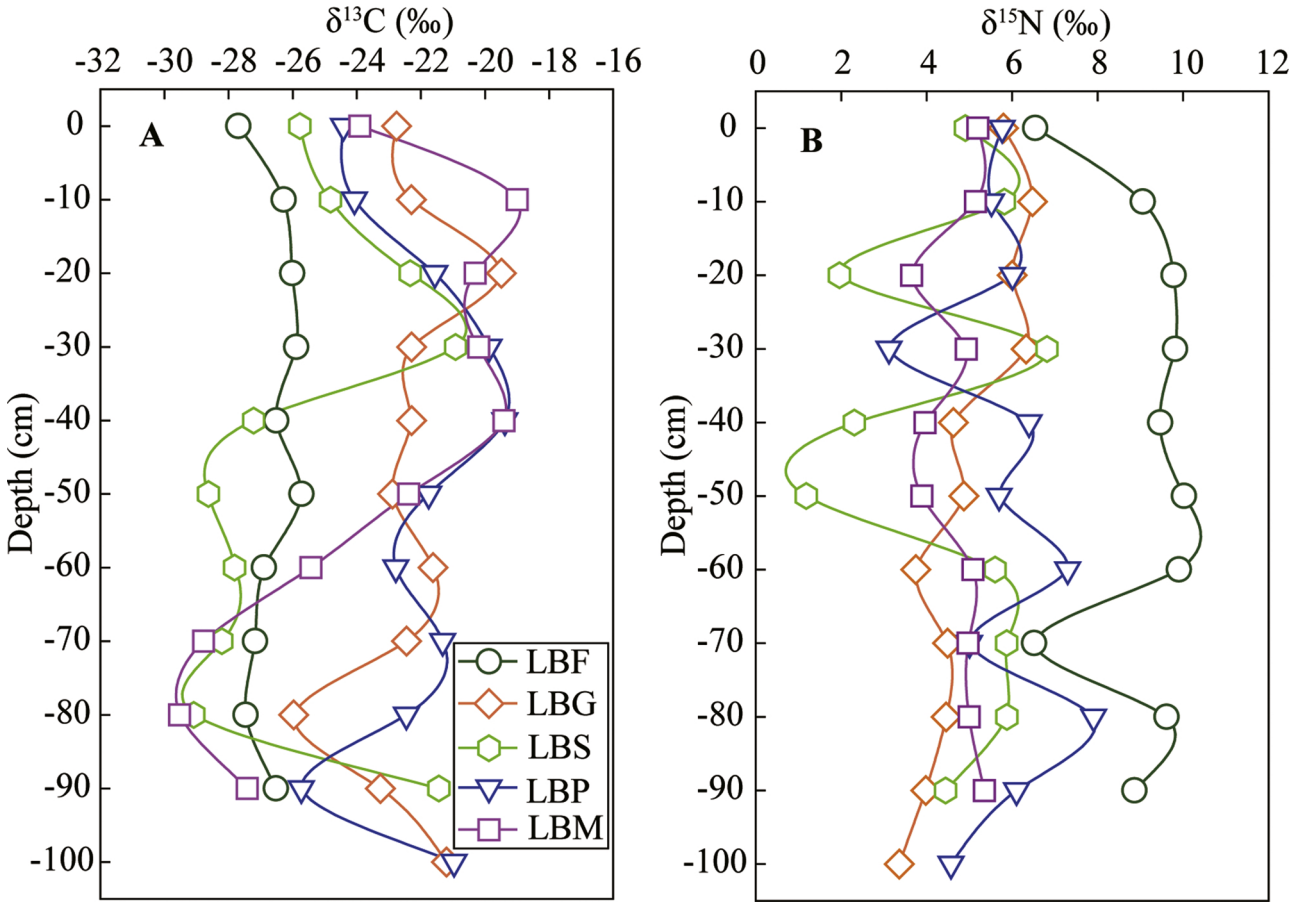

Fig. 6. Changes in $\delta^{13}C$ values (A) and $\delta^{15}N$ values (B) of SOM along soil depth in the five soil profiles. SOM, soil organic matter; LBF, the site in native forest land; LBG, the site in grass land; LBS, the site in shrub land; LBM, the site in maize land; LBP, the site in paddy land.

$\delta^{13}C$ values of SOM generally increase by 1‰ ~ 3‰ with increasing soil depth under mature C_3 forest (Chen et al., 2005), which is associated with ^{13}C-enriched microbial biomass and the preferred consumption of ^{13}C-depleted organic matters in decomposition process (Boutton et al., 1998; Neff et al., 2002; Peri et al., 2012; Nel et al., 2018). The organic matters in the subsoil undergo longer-term decomposition compared to that in the topsoil, which leads to the larger accumulation of ^{13}C in SOM. Thus, SOM decomposition mainly controlled the change in the $\delta^{13}C$ values of SOM in the LBF profile. However, relative large changes in the $\delta^{13}C$ values of SOM in other profiles were explained as dominant C_4 vegetation occurred in the past. Because C_3 and C_4 vegetation composition mainly determine the changes in the $\delta^{13}C$ of SOM when the land had occurred dominant vegetation alteration (Ellert and Janzen, 2006).

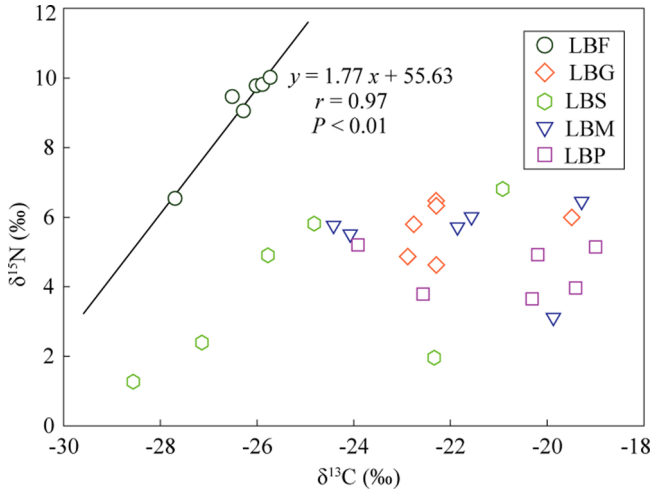

Fig. 7. Relationships between $\delta^{13}C$ values and $\delta^{15}N$ values of SOM from the five soil profiles at the 0 ~ 50 cm depth. The linear relationships under LBG, LBS, LBM, and LBP profiles were not credible ($P > 0.05$), thus the best-fit lines of them were not shown. SOM, soil organic matter; LBF, the site in native forest land; LBG, the site in grass land; LBS, the site in shrub land; LBM, the site in maize land; LBP, the site in paddy land.

From topsoil to the subsoil, the $\delta^{15}N$ values of SOM in LBF profile increased by 4‰, while that in other profiles fluctuated irregularly from 1‰ ~ 6‰ (Fig. 7). The mineralization of SON generally produces ^{15}N-depleted NH_4^+ while accumulates ^{15}N-enriched N in microorganism (Krull et al., 2006). Subsequent nitrification that NH_4^+ transforms into NO_3^- by nitrifying bacteria further depletes ^{15}N in NO_3^- (Krull et al., 2006). The microbes in both mineralization and nitrification preferentially fix ^{15}N, and SOM mainly consists of dead microbes after heavy consumption of plant debris (Craine et al., 2015). In native forest land, ^{15}N-depleted inorganic N leaves the soils through sufficiently assimilating by plant root, resulting in ^{15}N-enriched SOM in residual organic matters (Nadelhoffer and Fry, 1988; Krull et al., 2006). Reduced plant biomass in grass land and shrub land leads to an incomplete absorption of ^{15}N-depleted inorganic N, and redundant inorganic N is reassimilated into microbes, thus the $\delta^{15}N$ values of SOM under the transformed lands is lower compared to native forest land. In farm lands, redundant ^{15}N-depleted NO_3^- derived from N-fertilizer ($\delta^{15}N$ is ~ 0‰, Choi et al., 2017) is leached downward and assimilated by fungi (Hobbie and Ouimette, 2009), which results in ^{15}N-depleted SOM in the subsoils. However, there were not significantly lower $\delta^{15}N$ values in the soils of farmland (LBM and LBP) compared to that under

grass land (LBG) and shrub land (LBS), which means that the effect of ^{15}N-depleted N-fertilizer on $\delta^{15}N$ composition of SOM can be ignored. The loss of ^{15}N-depleted NO_3^- is considered as an important way to increase $\delta^{15}N$ value at depth (Krull et al., 2006). Commonly, the loss of NO_3^- under forest land is the least, which means that ^{15}N-depleted inorganic N is more easily preserved in the soil-plant system. Therefore, the larger $\delta^{15}N$ values in the native forest land (LBF) compared to other transformed lands only is explained by more sufficiently assimilation by plant root (i.e. N utilization efficiency). Moreover, the conversion of forest land to grass land or farm land can decrease soil N utilization efficiency. Additionally, the assimilation process against ^{15}N-depleted inorganic N in the subsoil results in ^{15}N enrichment in SOM with increasing soil depth in the forest land. When the lands have not occurred land use change (i.e., the alteration of C_3/C_4 vegetation composition) and fertilizer application, both the $\delta^{15}N$ and $\delta^{13}C$ values of SOM generally increase with increasing soil depth, which mainly depends on SOM decomposition (Nadelhoffer and Fry, 1988; Krull et al., 2006). In addition, when soil N utilization efficiency is sufficient, there is a high consistency of ^{13}C and ^{15}N enrichment with SOM decomposition degree as shown the well linear relationship between $\delta^{15}N$ values and $\delta^{13}C$ values of SOM in native forest land (LBF profile). Thus, it can be inferred that the coupling of C-N isotope fractionation is easily observed in the C_3 forest ecosystem with high N utilization efficiency.

5. Conclusions

This study indicated that SOC and SON contents were significantly reduced when forest land converts into grass land or farm land in the Maolan karst area, and the effects mainly focus on the 0 ~ 20 cm depth layer. The contents of SOC and SON decreased exponentially with increasing soil depth under all land use types, and showed inverse trends with soil pH. The C/N ratio, $\delta^{13}C$, and $\delta^{15}N$ values of SOM in the lands occurred land use change showed intensively irregular fluctuation along soil profiles compared to these in native forest land. The results suggested that the chaotic signals of single $\delta^{13}C$ and $\delta^{15}N$ of SOM in the soil profiles under land use change restricted the indication of SOM sources and transformation processes. Only in the soils under undisturbed C_3 plant forest land, the $\delta^{13}C$, and $\delta^{15}N$ of SOM showed a positive relationship, resulting from full plant-absorption of ^{15}N-depleted inorganic nitrogen derived from SOM mineralization. Thus, the coupling of C-N isotope fractionation more likely occurs in the C_3 forest ecosystem with high N utilization efficiency, and the replacement of native forest by farm land or grass land will reduce soil N utilization efficiency. We suggest that decreasing agricultural activities and increasing vegetation coverage are the keys to reducing the N loss in the karst ecosystems.

Declaration of competing interest

The authors declare no conflict of interest.

Acknowledgements

This work was jointly supported by the National Natural Science Foundation of China (No. 41325010; 41661144029; 41571130042). The authors gratefully acknowledge Fushan Li for sampling and laboratory assistance.

References

Amundson, R., Berhe, A.A., Hopmans, J.W., Olson, C., Sztein, A.E., Sparks, D.L., 2015. Soil science. Soil and human security in the 21st century. Science 348, 1261071. https://doi.org/10.1126/science.1261071.

Aryal, D.R., Morales Ruiz, D.E., Marroquín, T., Noé, C., Pinto Ruiz, R., Guevara Hernández, F., Venegas Venegas, J.A., Ponce Mendoza, A., Villanueva López, G., Casanova Lugo, F., Jonapa, F.J., Sanabria, M.C.A.V., Aguilar, A.A., Chi, I.E., 2018. Soil organic carbon depletion from forests to grasslands conversion in Mexico: a review. Agriculture 8, 181. https://doi.org/10.3390/agriculture8110181.

Bojko, O., Kabala, C., 2017. Organic carbon pools in mountain soils—sources of variability and predicted changes in relation to climate and land use changes. Catena 149, 209–220. https://doi.org/10.1016/j.catena.2016.09.022.

Boutton, T.W., Archer, S.R., Midwood, A.J., Zitzer, S.F., Bolb, R., 1998. $\delta^{13}C$ values of soil organic carbon and their use in documenting vegetation change in a subtropical savanna ecosystem. Geoderma 82, 5–41. https://doi.org/10.1016/j.regpep.2014.08.004.

Chaopricha, N.T., Marín-Spiotta, E., 2014. Soil burial contributes to deep soil organic carbon storage. Soil Biol. Biochem. 69, 251–264. https://doi.org/10.1016/j.soilbio.2013.11.011.

Chen, Q.Q., Sun, Y.M., Shen, C.D., Peng, S.L., Yi, W.X., Li, Z.A., Jiang, M.T., 2002. Organic matter turnover rates and CO_2 flux from organic matter decomposition of mountain soil profiles in the subtropical area, south China. Catena 49, 217–229 https://doi.org/10.1016/s0341-8162 02 00044-00049.

Chen, Q.Q., Shen, C.D., Sun, Y.M., Peng, S.L., Yi, W.X., Li, Z.A., Jiang, M.T., 2005. Spatial and temporal distribution of carbon isotopes in soil organic matter at the Dinghushan Biosphere Reserve, South China. Plant Soil 273, 115–128. https://doi.org/10.1007/s11104-004-7245-y.

Choi, W.J., Kwak, J.H., Lim, S.S., Park, H.J., Chang, S.X., Lee, S.M., Arshad, M.A., Yun, S.I., Kim, H.Y., 2017. Synthetic fertilizer and livestock manure differently affect $\delta^{15}N$ in the agricultural landscape: A review. Agr. Ecosyst. Environ. 237, 1–15. https://doi.org/10.1016/j.agee.2016.12.020.

Conen, F., Zimmermann, M., Leifeld, J., Seth, B., Alewell, C., 2008. Relative stability of soil carbon revealed by shifts in $\delta^{15}N$ and C: N ratio. Biogeosciences 5, 123–128. https://doi.org/10.5194/bg-5-123-2008.

Craine, J.M., Brookshire, E.N.J., Cramer, M.D., Hasselquist, N.J., Koba, K., Marin-Spiotta, E., Wang, L., 2015. Ecological interpretations of nitrogen isotope ratios of terrestrial plants and soils. Plant Soil 396, 1–26. https://doi.org/10.1007/s11104-015-2542-1.

Deng, L., Shangguan, Z.P., 2017. Afforestation drives soil carbon and nitrogen changes in China. Land Degrad. Dev. 28, 151–165. https://doi.org/10.1002/ldr.2537.

Ellert, B.H., Janzen, H.H., 2006. Long-term biogeochemical cycling in agroecosystems inferred from ^{13}C, ^{14}C and ^{15}N. J. Geochem. Explor. 88, 198–201. https://doi.org/10.1016/j.gexplo.2005.08.038.

Fierer, N., Schmiel, J.P., Holden, P.A., 2003. Variations in microbial community composition through two soil depth profiles. Soil Biol. Biochem. 35, 167–176 https://doi.org/10.1016/s0038-0717 02 00251-1.

Gallowy, J.N., Asner, G., Boyer, E.W., Capone, D.G., Cleveland, C.C., Dentener, F.J., Greene, P., Holland, E., Howarth, R.W., Karl, D.M., Michaels, A.F., Seizinger, S.P., Toensend, A.R., Vöosmarty, C.J., 2005. Global and regional nitrogen cycles: past, present and future. Biogeochemistry 70, 153–226. https://doi.org/10.1007/s10533-004-0370-0.

Gao, Y., He, N.P., Yu, G.R., Chen, W.L., Wang, Q.F., 2014. Long-term effects of different land use types on C, N, and P stoichiometry and storage in subtropical ecosystems: a case study in China. Ecol. Eng. 67, 171–181. https://doi.org/10.1016/j.ecoleng.2014.03.013.

Gelaw, A.M., Singh, B.R., Lal, R., 2015. Organic carbon and nitrogen associated with soil aggregates and particle sizes under different land uses in Tigray, Northern Ethiopia. Land Degrad. Dev. 26, 690–700. https://doi.org/10.1002/ldr.2261.

Han, G.L., Li, F.S., Tang, Y., 2015. Variations in soil organic carbon contents and isotopic compositions under different land uses in a typical karst area in Southwest China. Geochem. J. 49, 63–71. https://doi.org/10.2343/geochemj.2.0331.

Han, G.L., Li, F.S., Tang, Y., 2017. Organic matter impact on distribution of rare earth elements in soil under different land uses. Clean-Soil Air Water 45, 1600235. https://doi.org/10.1002/clen.201600235.

Han, G., Song, Z., Tang, Y., Wu, Q., Wang, Z., 2019. Ca and Sr isotope compositions of rainwater from Guiyang city, Southwest China: Implication for the sources of atmospheric aerosols and their seasonal variations. Atmos. Environ. 214, 116854. https://doi.org/10.1016/j.atmosenv.2019.116854.

Hilton, R.G., Galy, A., West, A.J., Hovius, N., Roberts, G.G., 2013. Geomorphic control on the $\delta^{15}N$ of mountain forests. Biogeosciences 10, 1693–1705. https://doi.org/10.5194/bg-10-1693-2013.

Hobbie, E.A., Hogberg, P., 2012. Nitrogen isotopes link mycorrhizal fungi and plants to nitrogen dynamics. New Phytol. 196, 367–382. https://doi.org/10.1111/j.1469-8137.2012.04300.x.

Hobbie, E.A., Ouimette, A.P., 2009. Controls of nitrogen isotope patterns in soil profiles. Biogeochemistry 95, 355–371. https://doi.org/10.1007/s10533-009-9328-6.

Hogberg, P., 1997. Tansley review No 95 ^{15}N natural abundance in soil—plant systems. New Phytol. 137, 179–203. https://doi.org/10.1046/j.1469-8137.1997.00808.x.

Hogberg, P., Johannisson, C., 1993. ^{15}N abundance of forests in correlated with losses of nitrogen. Plant Soil 157, 147–150. https://doi.org/10.1007/bf00038758.

Houlton, B.Z., Sigman, D.M., Hedin, L.O., 2006. Isotopic evidence for large gaseous nitrogen losses from tropical rainforests. Proc. Natl. Acad. Sci. USA 103, 8745–8750. https://doi.org/10.1073/pnas.0510185103.

Jobbagy, E.G., Jackson, R.B., 2000. The vertical distribution of soil organic carbon and its relation to climate and vegetation. Ecol. Appl. 10, 423–436. https://doi.org/10.2307/2641104.

Krull, E.S., Bestland, E.A., Skjemstad, J.O., Parr, J.F., 2006. Geochemistry ($\delta^{13}C$, $\delta^{15}N$, ^{13}C NMR) and residence times (^{14}C and OSL) of soil organic matter from red-brown earths of South Australia: Implications for soil genesis. Geoderma 132, 344–360. https://doi.org/10.1016/j.geoderma.2005.06.001.

Lal, R., 2004. Soil carbon sequestration impacts on global climate change and food security. Science 304, 1623–1627. https://doi.org/10.1126/science.1097396.

Liu, W.G., Wei, J., Cheng, J.M., Li, W.J., 2014. Profile distribution of soil inorganic carbon along a chronosequence of grassland restoration on a 22-year scale in the Chinese Loess Plateau. Catena 121, 321–329. https://doi.org/10.1016/j.catena.2014.05.019.

Liu, X., Ma, J., Ma, Z.W., Li, L.H., 2017. Soil nutrient contents and stoichiometry as affected by land-use in an agro-pastoral region of northwest China. Catena 150, 146–153. https://doi.org/10.1016/j.catena.2016.11.020.

Liu, M., Han, G.L., Zhang, Q., 2019a. Effects of soil aggregate stability on soil organic carbon and nitrogen under land use change in an erodible region, Southwest China. Int. J. Env. Res. Pub. He. 16, 3809. https://doi.org/10.3390/ijerph16203809.

Liu, M., Han, G.L., Zhang, Q., Song, Z.L., 2019b. Variations and indications of $\delta^{13}C_{SOC}$ and $\delta^{15}N_{SON}$ in soil profiles in karst Critical Zone Observatory (CZO), Southwest China. Sustainability 11, 2144. https://doi.org/10.3390/su11072144.

Liu, M., Han, G., Zhang, Q., 2020. Effects of agricultural abandonment on soil aggregation, soil organic carbon storage and stabilization: results from observation in a small karst catchment, Southwest China. Agr. Ecosyst. Environ. 288, 106719. https://doi.org/10.1016/j.agee.2019.106719.

Mariotti, A., 1983. Atmospheric nitrogen is a reliable standard for natural ^{15}N abundance measurements. Nature 303, 685–687. https://doi.org/10.1038/303685a0.

Mariotti, A., Germon, J.C., Hubert, P., Kaiser, P., Letolle, R., Tardieux, A., Tardieux, P., 1981. Experimental determination of nitrogen kinetic isotopes fractionation: Some principles; illustration for the denitrification and nitrification processes. Plant Soil 62, 413–430. https://doi.org/10.1007/bf02374138.

Meng, L., Ding, W., Cai, Z., 2005. Long-term application of organic manure and nitrogen fertilizer on N_2O emissions, soil quality and crop production in a sandy loam soil. Soil Biol. Biochem. 37, 2037–2045. https://doi.org/10.1016/j.soilbio.2005.03.007.

Midwood, A.J., Boutton, T.W., 1998. Soil carbonated decomposition by acid has little effect on $\delta^{13}C$ of organic matter. Soil Biol. Biochem. 30, 1301–1307 https://doi.org/10.1016/S0038-0717 98 00030-00033.

Nadelhoffer, K.J., Fry, B., 1988. Controls on natural nitrogen-15 and carbon-13 abundance in forest soil organic matter. Soil Sci. Soc. Am. J. 52, 1633–1640. https://doi.org/10.2136/sssaj1988.03615995005200060024x.

National Soil Survey Office (NSSO), 1998. Soil of China. China Agriculture Press, Beijing.

Navas, A., Gaspar, L., Quijano, L., López-Vicente, M., Machín, J., 2012. Patterns of soil organic carbon and nitrogen in relation to soil movement under different land uses in mountain fields (South Central Pyrenees). Catena 94, 43–52. https://doi.org/10.1016/j.catena.2011.05.012.

Neff, J.C., Townsend, A.R., Gleixner, G., Lehman, S.J., Turnbull, J., Bowman, W.D., 2002. Variable effects of nitrogen additions on the stability and turnover of soil carbon. Nature 419, 915–917. https://doi.org/10.1038/nature01136.

Nel, J.A., Craine, J.M., Cramer, M.D., 2018. Correspondence between $\delta^{13}C$ and $\delta^{15}N$ in soils suggests coordinated fractionation processes for soil C and N. Plant Soil 423, 1–15. https://doi.org/10.1007/s11104-017-3500-x.

Oktaba, L., Paziewski, K., Kwasowski, W., Kondras, M., 2014. The effect of urbanization on soil properties and soil organic carbon accumulation in topsoil of Pruszków – a medium-sized city in the Warsaw Metropolitan Area, Poland. Soil Sci. Annual 65, 10–17. https://doi.org/10.2478/ssa-2014-0002.

Peri, P.L., Ladd, B., Pepper, D., Bonser, S.P., Laffan, S.W., Amelung, W., 2012. Carbon ($\delta^{13}C$) and nitrogen ($\delta^{15}N$) stable isotope composition in plant and soil in Southern Patagonia's native forests. Glob. Change Biol. 18, 311–321. https://doi.org/10.1111/j.1365-2486.2011.02494.x.

Portl, K., Zechmeister-Boltenstern, S., Wanek, W., Ambus, P., Berber, T.W., 2007. Natural ^{15}N abundance of soil N pools and N_2O reflect the nitrogen dynamics of forest soils. Plant Soil 295, 79–94. https://doi.org/10.1007/s11104-007-9264-y.

Rasmussen, C., 2006. Distribution of soil organic and inorganic carbon pools by biome and soil taxa in Arizona. Soil Sci. Soc. Am. J. 70, 256–265. https://doi.org/10.2136/sssaj2005.0118.

Rumpel, C., Kogel-Knabner, I., 2011. Deep soil organic matter—a key but poorly understood component of terrestrial C cycle. Plant Soil 338, 143–158. https://doi.org/10.1007/s11104-010-0391-5.

Schmidt, M.W.I., Torn, M.S., Abiven, S., Dittmar, T., Guggenberger, G., Janssens, I.A., Kleber, M., Kogel-Knabner, I., Lehmann, J., Manning, D.A.C., Nannipieri, P., Rasse, D.P., Weiner, S., Trumbore, S.E., 2011. Persistence of soil organic matter as an ecosystem property. Nature 478, 49–56. https://doi.org/10.1038/nature10386.

Smith, P., House, J.I., Bustamante, M., Sobocka, J., Harfer, R., Pan, G., West, P.C., Clark, J.M., Adhya, T., Rumpel, C., Paustian, K., Kuikman, P., Cotrufo, M.F., Elliott, J.A., Mcdowell, R., Griffiths, R.I., Asakawa, S., Bondeau, A., Jain, A., Meersmans, J., Pugh, T.A.M., 2016. Global change pressures on soils from land use and management. Glob. Change Biol. 22, 1008–1028. https://doi.org/10.1111/geb.13068.

Staddon, P.L., 2004. Carbon isotopes in functional soil ecology. Trends Ecol. Evol. 19, 148–154. https://doi.org/10.1016/j.tree.2003.12.003.

Templer, P.H., Arthur, M.A., Lovett, G.M., Weathers, K.C., 2007. Plant and soil natural abundance $\delta^{15}N$: indicators of relative rates of nitrogen cycling in temperate forest ecosystems. Oecologia 153, 99–406. https://doi.org/10.1007/s00442-007-0746-7.

Tesfaye, M.A., Bravo, F., Ruiz-Peinado, R., Pando, V., Bravo-Oviedo, A., 2016. Impact of changes in land use, species and elevation on soil organic carbon and total nitrogen in Ethiopian Central Highlands. Geoderma 261, 70–79. https://doi.org/10.1016/j.geoderma.2015.06.022.

Trumbore, S.E., Davidson, E.A., Decamargo, P.B., Nepstad, D.C., Martinelli, L.A., 1995. Belowground cycling of carbon in forests and pastures of eastern Amazonia. Global Biogeochem. Cycles 9, 515–528. https://doi.org/10.1029/95gb02148.

Wallander, H., Morth, C.M., Giesler, R., 2009. Increasing abundance of soil fungi is a driver for ^{15}N enrichment in soil profiles along a chronosequence undergoing isostatic rebound in northern Sweden. Oecologia 160, 87–96. https://doi.org/10.1007/s00442-008-1270-0.

Wang, S.J., Liu, Q.M., Zhang, D.F., 2004. Karst rocky desertification in southwestern China: geomorphology, landuse, impact and rehabilitation. Land Degrad. Dev. 15, 115–121. https://doi.org/10.1002/ldr.592.

Wang, W., Sardans, J., Zeng, C., Zhong, C., Penuelas, J., 2014. Responses of soil nutrient concentrations and stoichiometry to different human land uses in a subtropical tidal wetland. Geoderma 232, 459–470. https://doi.org/10.1016/j.geoderma.2014.06.004.

Zeng, J., Yue, F.J., Wang, Z.J., Wu, Q., Qin, C.Q., Li, S.L., 2019. Quantifying depression trapping effect on rainwater chemical composition during the rainy season in karst agricultural area, southwestern China. Atmos. Environ. 218, 116998. https://doi.org/10.1016/j.atmosenv.2019.116998.

Zeng, J., Han, G., Wu, Q., Tang, Y., 2020a. Effects of agricultural alkaline substances on reducing the rainwater acidification: insight from chemical compositions and calcium isotopes in a karst forests area. Agr. Ecosyst. Environ. 290, 106782. https://doi.org/10.1016/j.agee.2019.106782.

Zeng, J., Yue, F.J., Li, S.L., Wang, Z.J., Qin, C.Q., Wu, Q.X., Xu, S., 2020b. Agriculture driven nitrogen wet deposition in a karst catchment in southwest China. Agr. Ecosyst. Environ. 294, 106883. https://doi.org/10.1016/j.agee.2020.106883.

Zhang, C., Liu, G.B., Xue, S., Sun, C.L., 2013. Soil organic carbon and total nitrogen storage as affected by land use in a small watershed of the Loess Plateau. China. Eur. J. Soil Biol. 54, 16–24. https://doi.org/10.1016/j.ejsobi.2012.10.007.

Zhang, J., Wang, X.J., Wang, J.P., 2014. Impact of land use change on profile distributions of soil organic carbon fractions in the Yanqi Basin. Catena 115, 79–84. https://doi.org/10.1016/j.catena.2013.11.019.

Zhang, Q., Han, G.L., Liu, M., Liang, T., 2019. Spatial distribution and controlling factors of heavy metals in soils from Puding Karst Critical Zone Observatory, southwest China. Environ. Earth Sci. 78, 279. https://doi.org/10.1007/s12665-019-8280-6.

Zhu, S.F., Liu, C.Q., 2006. Vertical patterns of stable carbon isotope in soils and particle-size fractions of karst areas, Southwest China. Environ. Geol. 50, 1119–1127. https://doi.org/10.1007/s00254-006-0285-2.